2022 EAGE ANNUAL
83RD CONFERENCE & EXHIBITION
MADRID I SPAIN

EFFECTS OF NONREPEATABILITY ON TIME-LAPSE FULL-WAVEFORM INVERSION

A. Mardan[1], B. Giroux[1], G. Fabien-Ouellet[2]

[1] INRS; [2] Polytechnique de Montréal

Summary

Full waveform inversion (FWI) is a data-fitting process based on full-waveform modeling and a proven method to estimate the (visco)elastic moduli of the subsurface at high resolution. Time-lapse FWI (TL-FWI) used this technique to estimate the 4D changes of the earth's property based on the difference between the seismic data acquired in different vintages. However, nonrepeatability (NR) in the two surveys can deteriorate the quality of the results. Although survey design and different 4D processing techniques can decrease the effects of NR, this problem is not avoidable. In this study, we show the effects of different NR on the seismic data and two accurate time-lapse FWI methods. Weighted-averaged and a modified version of the central-difference TL-FWI are assessed to analyze their efficiency to address the different sources of NR. Although without NR, these two methods provide very accurate and similar results, by the presence of NR, the weighted-averaged TL-FWI estimates a much more accurate time-lapse image than the implemented central-difference method.

Effects of nonrepeatability on time-lapse full-waveform inversion

Introduction

Full waveform inversion (FWI) is a data-fitting process based on full-waveform modeling to estimate the physical properties of the Earth (Tarantola, 1984). Because of its capacity to recover change of (visco)elastic modulus at potential high resolution, FWI has been increasingly used in time-lapse manner for reservoir monitoring (Watanabe et al., 2005; Fabien-Ouellet et al., 2017; Zhou and Lumley, 2021b). Time-lapse FWI (TL-FWI) estimates the 4D changes based on the difference between the seismic data acquired in different vintages. Thereby, any source of nonrepeatability (NR) in the two surveys can deteriorate the quality of the results. Various 4D processing techniques have been proposed to address this problem (Kiyashchenko et al., 2020; Rickett and Lumley, 2001). Although these techniques decrease the effects of NR on the results, undesirable artifacts cannot be eliminated completely. Survey design can also help reduce NR artifacts. For instance, a permanent setup of ocean bottom cable (OBC) can decrease the NR in the first place (Raknes and Arntsen, 2015). Nevertheless, long-term subsidence and uplifting of the seafloor can cause NR to occur in the presence of OBC. In fact, variation of seawater velocity due to temperature and salinity is another source of NR that OBC acquisition is not capable to suppress (Zhou and Lumley, 2021b).

Various studies have been carried out to assess the effects of time-lapse noises on migrated images and the resilience of different migration algorithms (L'Heureux and Gherasim, 2015; Gherasim et al., 2016). Different researchers have also analyzed NR and its effects on the efficacy of TL-FWI methods. Kamei and Lumley (2017) studied the effects of NR on parallel, double-difference (Watanabe et al., 2005), and cascaded (Routh et al., 2012) inversion and stated that the cascaded inversion provides the most accurate results. Zhou and Lumley (2021b) highlighted the strong effects of source-receiver positioning error and water velocity variation. They also showed the robustness of the central-difference method (Zhou and Lumley, 2021a) over parallel and double-difference inversion.

The objective of this study is to analyze the effects of NR on the efficiency of a modified version of central-difference (Zhou and Lumley, 2021a) and the weighted-averaged inversion (Mardan et al., 2022b). The considered NR is due to source-receiver positioning, constant tide, and variability of water velocity. In the next section, we discuss the theory of TL-FWI and the mentioned TL-FWI methods. Then the effects of NR are examined using the Marmousi model. We should mention that this study was performed with algorithms implemented in PyFWI (Mardan et al., 2022a).

Methodology

FWI can be implemented in the time domain by minimizing the difference between observed and estimated data. The cost function, $\mathcal{C}(\mathbf{m})$, can be expressed as

$$\min_{m\in\mathbb{M}} \mathcal{C}(\mathbf{m}) = \frac{1}{2}\|F(\mathbf{m}) - d\|_2^2 \tag{1}$$

where F is the forward modeling operator, d is representing observed data and $\mathbf{m}$ denotes the Earth's properties belonging to the model space $\mathbb{M}$. For TL-FWI, equation 1 can be used for inverting the seismic data of different vintages independently. In this case, baseline and monitor models ($\mathbf{m}_b$ and $\mathbf{m}_m$) are estimated individually which is the most basic method for TL-FWI. To improve the accuracy of time-lapse estimates, a variety of strategies have been proposed (Maharramov and Biondi, 2014; Fabien-Ouellet et al., 2017; Zhou and Lumley, 2021a; Mardan et al., 2022b). However, the focus of this study is on weighted-averaged (Mardan et al., 2022b) and modified central-difference method (Zhou and Lumley, 2021a). Weighted-averaged method (Figure 1a) works based on equation 1 and includes three independent runs of FWI to obtain two models of the baseline and one monitor model. Based on these three estimates, one reverse ($\Delta\mathbf{m}^-$) and one forward bootstraps ($\Delta\mathbf{m}^+$) are computed,

$$\Delta\mathbf{m}^- = \mathbf{m}_m - \mathbf{m}_b, \tag{2a}$$

$$\Delta\mathbf{m}^+ = \mathbf{m}'_b - \mathbf{m}_m, \tag{2b}$$

where subscripts b and m represents baseline and monitor models respectively and $\mathbf{m}'_b$ is the second estimate of the baseline model. The final estimate of the 4D image is the weighted average of these two bootstraps,

$$\Delta\mathbf{m} = \frac{\alpha\Delta\mathbf{m}^- + \Delta\mathbf{m}^+}{1+\alpha}. \tag{3}$$

The implemented central-difference method (Figure 1b) on the other hand, employs four runs of FWI. This method estimates one set of baseline and monitor models and uses their average as the initial model for implementing another parallel inversion. Then, a second set of baseline and monitor models is estimated ($\mathbf{m}'_b$ and $\mathbf{m}'_m$). Ultimately the final 4D response is obtained as

$$\Delta\mathbf{m} = \frac{\Delta\mathbf{m}^- + \Delta\mathbf{m}^+}{2}. \tag{4}$$

Weighted-averaged and central-difference techniques are among the most accurate approaches of TL-FWI in the absence of NR. Nevertheless, NR is a common issue in monitoring. In the next section, the impacts of NR on the results and on the efficiency of these methods are examined.

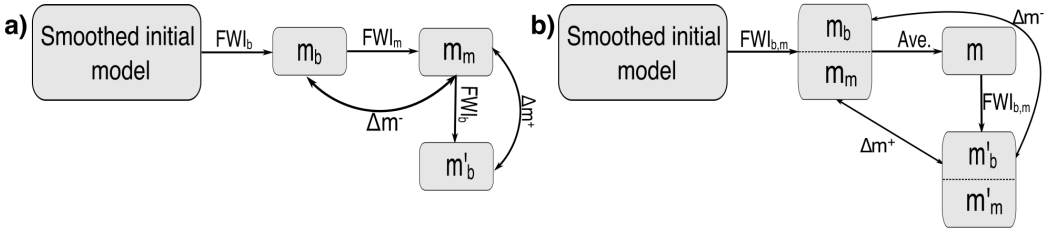

Figure 1 *The flowcharts of (a) weighted-averaged and (b) modified central-difference TL-FWI.*

Example

To examine the effects of NR on the TL-FWI, we use a portion of the Marmousi model. To generate the baseline model, two reservoirs are filled with their background properties (Figure 2a). The original model is used as the monitor model (Figure 2b) and the baseline is smoothed to generate the initial model (Figure 2c). Figure 2d represents the absolute value of 4D changes in percent.

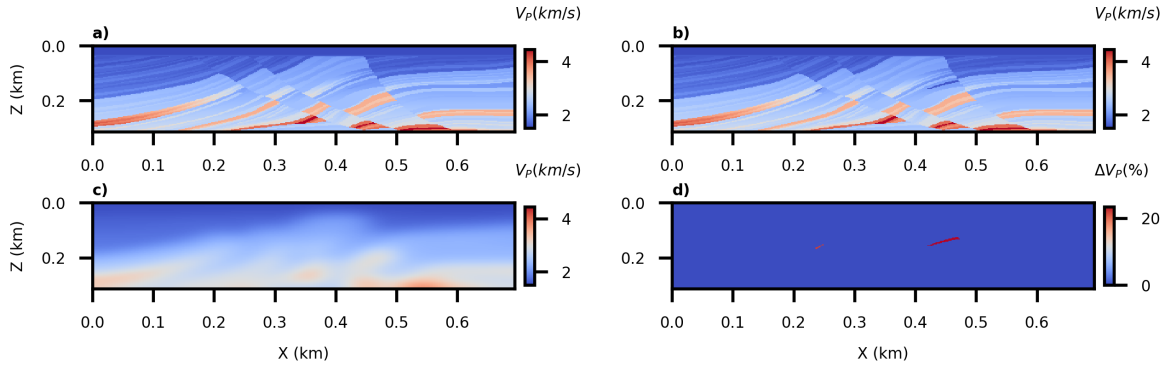

Figure 2 *Marmousi model is used to study the effects of NR. (a) Baseline and (b) monitor P-wave velocity models. (c) The smoothed initial model. (d) The absolute value of percent changes.*

For practical reasons, baseline shot and ocean bottom node (OBN) positions cannot be repeated perfectly (Zhou and Lumley, 2021b). To analyze the effects of NR, the two TL-FWI methods are tested in different scenarios. In the first scenario, two surveys are repeated perfectly. In the second case, sources and receivers are displaced by 1 m. Then a constant tide with a height of 1 m is assumed. For the fourth situation, the velocity of water in the shallow part (10 m) is increased by 2%.

One observed shot gather from the central source of the baseline and monitor data in different situations are shown in Figure 3(a-e). These data are obtained in a surface acquisition with 12 isotropic explosive sources with considering a perfectly matched layer (PML) around the model. For this study, we used a Ricker wavelet with a peak frequency of 15 Hz. The discrepancy of different sections with the baseline data is shown in Figure 3(f-i). As shown, NR can generate significant discrepancies in the data. In the next section, the efficiency of TL-FWI methods to address this problem is analyzed.

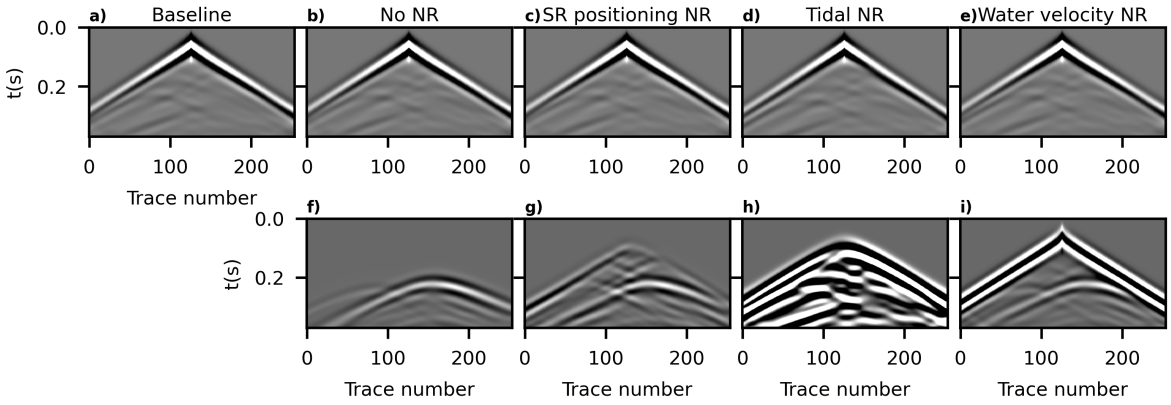

Figure 3 *(a-e) The observed data from (a) baseline and (b-e) monitor models using different scenarios of NR with color a scale based on the baseline data. (f-i) The discrepancy between the baseline and each monitor data with a color scale based on the discrepancy in perfectly repeated acquisition. (b and f) Absence of NR, (c and g) source/receiver (SR) positioning NR, (d and h) tidal NR, and (e and i) NR due to water velocity variation.*

Results

The datasets shown in Figure 3 are inverted with the weighted-averaged and the modified central-difference inversion to assess their capacity. The result and the root mean square error (*RMSE*) of its discrepancy from the true 4D anomaly are presented in Figure 4. This figure shows that NR has a significant effect on TL-FWI and that each time-lapse strategy can cope with this problem differently, with a clear advantage for the weighted-averaged inversion. Although water level variation generates the strongest effects (with artifacts having amplitudes comparable to the sought anomaly in the case of central-difference inversion), this problem can be dealt properly at the processing step. Besides, knowledge of seawater properties is required to address the problem of water velocity variation.

Conclusions

In this study, the effects of nonrepeatability in time-lapse full-waveform inversion are analyzed. We show that a small variation of water velocity deteriorates the estimated 4D images and good knowledge about the situation of seawater is required. Besides, different time-lapse methods cope with nonrepeatability differently and in this study, the weighted-averaged method showed less sensitivity to NR effects than cascaded-joint inversion. That is an additional point to the fact that the weighted-averaged method needs one run of full-waveform inversion less than the central-difference method and thereby, it is a faster method.

References

Fabien-Ouellet, G., Gloaguen, E. and Giroux, B. [2017] Time domain viscoelastic full waveform inversion. *Geophysical Journal International*, **209**(3), 1718–1734.

Gherasim, M., L'Heureux, E. and Lorenzo, Z. [2016] Evaluation and correction of sources of 4D noise using modeled ocean-bottom-node data. *The Leading Edge*, **35**(10), 880–886.

Kamei, R. and Lumley, D. [2017] Full waveform inversion of repeating seismic events to estimate time-

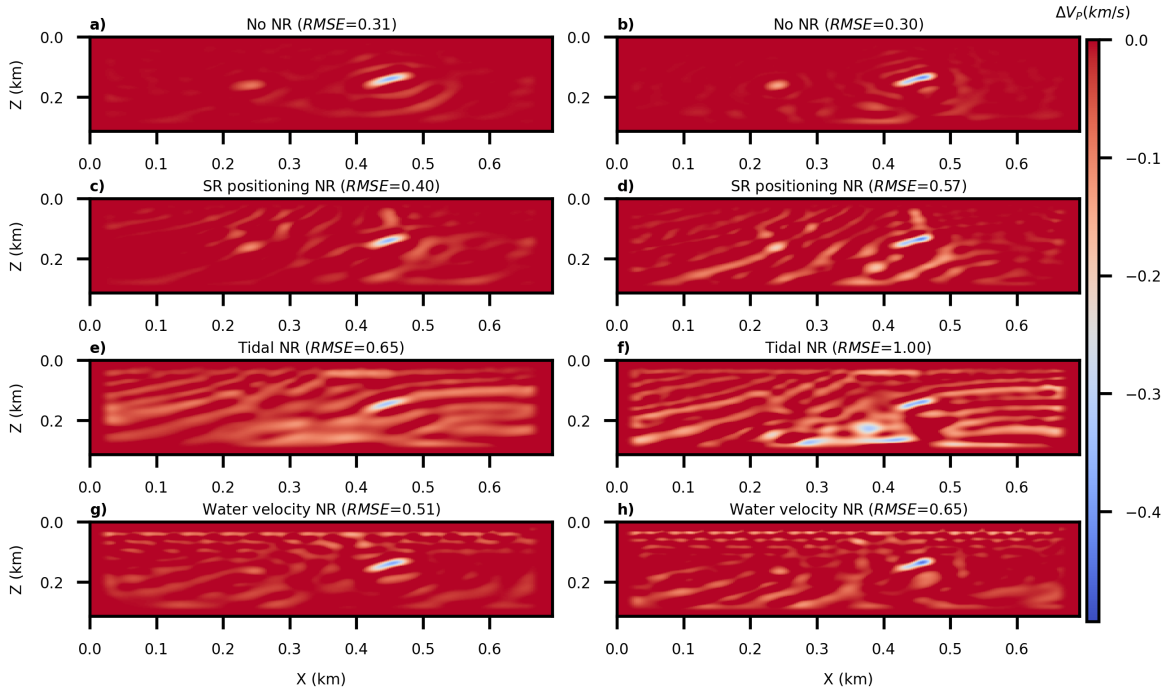

Figure 4 *Results of weighted-averaged (left column) and implemented central-difference (right column) methods in case of (a-b) no NR, (c-d) SR positioning NR, (e-f) tidal NR, and (f-g) NR due to water velocity variation.*

lapse velocity changes. *Geophysical Journal International*, **209**(2), 1239–1264.

Kiyashchenko, D., Wong, W.F., Cherief, D., Clarke, D., Duan, Y. and Hatchell, P. [2020] Unlocking seismic monitoring of stiff reservoirs with 4D OBN: a case study from Brazil pre-salt. In: *SEG Technical Program Expanded Abstracts 2020*, Society of Exploration Geophysicists, 3759–3763.

L'Heureux, E. and Gherasim, M. [2015] Evaluating the sources of 4D noise through controlled experiments with synthetic seismic data. In: *2015 SEG Annual Meeting*. OnePetro.

Maharramov, M. and Biondi, B. [2014] Robust joint full-waveform inversion of time-lapse seismic data sets with total-variation regularization. *arXiv: Geophysics*.

Mardan, A., Giroux, B. and Fabien-Ouellet, G. [2022a] PyFWI: A Python package for Full-Waveform Inversion (FWI).

Mardan, A., Giroux, B. and Fabien-Ouellet, G. [2022b] Time-Lapse Seismic Full Waveform Inversion Using Improved Cascaded Method. In: *2nd EAGE Conference on Seismic Inversion 2022*, 2022. European Association of Geoscientists & Engineers, 1–5.

Raknes, E.B. and Arntsen, B. [2015] A numerical study of 3D elastic time-lapse full-waveform inversion using multicomponent seismic data. *Geophysics*, **80**(6), R303–R315.

Rickett, J. and Lumley, D. [2001] Cross-equalization data processing for time-lapse seismic reservoir monitoring: A case study from the Gulf of Mexico. *Geophysics*, **66**(4), 1015–1025.

Routh, P., Palacharla, G., Chikichev, I. and Lazaratos, S. [2012] *Full Wavefield Inversion of Time-Lapse Data for Improved Imaging and Reservoir Characterization*. 1–6.

Tarantola, A. [1984] Inversion of seismic reflection data in the acoustic approximation. *Geophysics*, **49**(8), 1259–1266.

Watanabe, T., Shimizu, S., Asakawa, E. and Matsuoka, T. [2005] *Differential waveform tomography for time-lapse crosswell seismic data with application to gas hydrate production monitoring*. 2323–2326.

Zhou, W. and Lumley, D. [2021a] Central-difference time-lapse 4D seismic full-waveform inversion. *Geophysics*, **86**(2), R161–R172.

Zhou, W. and Lumley, D. [2021b] Nonrepeatability effects on time-lapse 4D seismic full-waveform inversion for ocean-bottom node data. *Geophysics*, **86**(4), R547–R561.